Relationship Between Nerve Fiber Layer Hemorrhages and Outcomes in Central Retinal Vein Occlusion

Adrian Au,[1] Assaf Hilely,[1,2] Jackson Scharf,[1] Frederic Gunnemann,[1,3] Derrick Wang,[1] Ismael Chehaibou,[1] Claudio Iovino,[4] Christelle Grondin,[1] Marie-Louise Farecki,[3] Khalil Ghasemi Falavarjani,[5] Nopasak Phasukkijwatana,[6] Marco Battista,[7] Enrico Borrelli,[7] Riccardo Sacconi,[7] Brittany Powell,[8] Grant Hom,[9] Tyler E. Greenlee,[9] Thais F. Conti,[9] Gerardo Ledesma-Gil,[10] Mehmet Yasin Teke,[11] Netan Choudhry,[12] Adrian T. Fung,[13] Valerie Krivosic,[14] Jiwon Baek,[15] Mee Yon Lee,[16] Yoshimi Sugiura,[10] Giuseppe Querques,[7] Enrico Peiretti,[4] Richard Rosen,[8] Won Ki Lee,[17] Lawrence A. Yannuzzi,[10] Dinah Zur,[2] Anat Loewenstein,[2] Daniel Pauleikhoff,[3] Rishi Singh,[9] Yasha Modi,[18] Jean Pierre Hubschman,[1] Michael Ip,[19] SriniVas Sadda,[19] K. Bailey Freund,[10] and David Sarraf[1,20]

[1]Stein Eye Institute, University of California, Los Angeles, California, United States
[2]Ophthalmology Division, Tel Aviv Sourasky Medical Center, Sackler Faculty of Medicine, Tel Aviv University, Tel Aviv, Israel
[3]Department of Ophthalmology, St. Franziskus-Hospital, Münster, Germany
[4]Department of Surgical Science, Eye Clinic, University of Cagliari, Cagliari, Italy
[5]Eye Research Center and Eye Department, Rassoul Akram Hospital, Iran University of Medical Sciences, Tehran, Iran
[6]Department of Ophthalmology, Faculty of Medicine Siriraj Hospital, Mahidol University, Bangkok, Thailand
[7]Department of Ophthalmology, Ospedale San Raffaele Scientific Institute University Vita-Salute San Raffaele, Milan, Italy
[8]Department of Ophthalmology, New York Eye and Ear Infirmary of Mount Sinai, New York, New York, United States
[9]Cole Eye Institute, Cleveland Clinic, Cleveland, Ohio, United States
[10]Vitreous Retina Macula Consultants of New York, New York, United States
[11]Ophthalmology Department, Ankara Ulucanlar Eye Training and Research Hospital, Ankara, Turkey
[12]Vitreous Retina Macula Specialists of Toronto, Toronto, Ontario, Canada
[13]Discipline of Ophthalmology, Westmead and Central Clinical Schools, University of Sydney; Department of Ophthalmology, Faculty of Medicine and Health Sciences, Macquarie University, Sydney, New South Wales, Australia
[14]Hôpital Lariboisière, AP-HP, Université Paris-Diderot, Sorbonne Paris Cité. France
[15]Department of Ophthalmology, Bucheon St. Mary's Hospital, College of Medicine, The Catholic University of Korea, Gyeonggi-do, Republic of Korea
[16]Department of Ophthalmology, Uijeongbu St. Mary's Hospital, College of Medicine, The Catholic University of Korea, Gyeonggi-do, Republic of Korea
[17]Retina Center, Nune Eye Hospital, Gangnam-gu, Seoul, Republic of Korea
[18]Department of Ophthalmology, New York University School of Medicine, New York, New York, United States
[19]Doheny Image Reading Center, Doheny Eye Institute, Los Angeles, California, United States
[20]VA Greater Los Angeles Healthcare System, Los Angeles, California, United States

Correspondence: David Sarraf, Stein Eye Institute, UCLA, 100 Stein Plaza, Los Angeles, CA 90095, USA; sarraf@jsei.ucla.edu, dsarraf@ucla.edu.

Received: December 5, 2019
Accepted: March 9, 2020
Published: May 27, 2020

Citation: Au A, Hilely A, Scharf J, et al. Relationship between nerve fiber layer hemorrhages and outcomes in central retinal vein occlusion. *Invest Ophthalmol Vis Sci.* 2020;61(5):54. https://doi.org/10.1167/iovs.61.5.54

Purpose. To evaluate the depth and pattern of retinal hemorrhage in acute central retinal vein occlusion (CRVO) and to correlate these with visual and anatomic outcomes.

Methods. Retinal hemorrhages were evaluated with color fundus photography and fluorescein angiography at baseline and follow-up. Snellen visual acuity (VA), central foveal thickness (CFT), extent of retinal ischemia, and development of neovascularization were analyzed.

Results. 108 eyes from 108 patients were evaluated. Mean age was 63.6 ± 16.1 years with a predilection for the right eye (73.1%). Average follow-up was 17.2 ± 19.2 months. Mean VA at baseline was 20/126 and 20/80 at final follow-up. Baseline ($P = 0.005$) and final VA ($P = 0.02$) in eyes with perivascular nerve fiber layer (NFL) hemorrhages were significantly worse than in eyes with deep hemorrhages alone. Baseline CFT was greater in the group with perivascular hemorrhages (826 ± 394 µm) compared to the group with deep hemorrhages alone (455 ± 273 µm, $P < 0.001$). The 10 disc areas of retinal ischemia was more common in patients with perivascular (80.0%) and peripapillary (31.3%) versus deep hemorrhages alone (16.1%, $P < 0.001$). Neovascularization of the iris was more common, although this difference was not significant, in the groups with peripapillary (14.3%) and perivascular (2.0%) NFL versus deep hemorrhages alone (0.0%).

Investigative Ophthalmology & Visual Science

Conclusions. NFL retinal hemorrhages at baseline correlate with more severe forms of CRVO, with greater macular edema, poorer visual outcomes, and greater risk of ischemia and neovascularization. This may be related to the organization of the retinal capillary plexus. The depth and pattern of distribution of retinal hemorrhages in CRVO may provide an easily identifiable early biomarker of CRVO prognosis.

Keywords: central retinal vein occlusion, nerve fiber layer hemorrhages, ischemia, neovascularization

Decades of research have been devoted to the identification of prognostic biomarkers that can predict central retinal vein occlusion (CRVO) visual outcomes and secondary complications. Initial studies identified poor baseline visual acuity, visual field, relative afferent pupillary defects, cotton wool spots and density of retinal hemorrhage as factors that portended a worse visual prognosis in eyes with CRVO.[1] The Central Vein Occlusion Study (CVOS) and other studies confirmed that baseline vision and confluent retinal hemorrhage, in addition to other factors such as afferent pupillary defect, correlated with worse outcomes including a greater risk of neovascular glaucoma.[2–5] The best way to assess CRVO outcomes may be to quantify the area of ischemia or non-perfusion with fluorescein angiography but interpretation was originally defined in the pre-widefield imaging era, can be limited by the presence of blood, and requires invasive dye injection.[6,7]

Advanced retinal imaging has provided greater insight into the evaluation of retinal vascular disease. Mild forms of CRVO may present with only middle retinal ischemia, not detectable with dye-based angiography, and identified as bands of hyperreflectivity in the inner nuclear layer referred to as paracentral acute middle maculopathy (PAMM).[8–12] These PAMM lesions may follow a perivenular distribution, best detected with en face optical coherence tomography (OCT), which may represent the mildest form of ischemic injury in CRVO[13,14] and the initial manifestation of the process recently referred to as the ischemic cascade.[15]

The progression of ischemic damage from the middle to the inner retinal layers in CRVO may share a parallel pathway with hemorrhage. Blood can be isolated in the Henle's fiber layer (HFL) as a result of systemic or local etiologies of elevated venous pressure including retinal vein occlusion.[16–18,39] Several studies have suggested that the intermediate and deep retinal capillary plexuses may represent the major level of venous outflow and it has therefore been proposed that ischemia and hemorrhage may first develop in the deeper layers of the retina.[14,15,19,20] With more severe venous occlusion, inner retinal ischemia and inner retinal hemorrhage may occur more frequently.[15]

We propose that the depth and pattern of distribution of retinal hemorrhages at presentation in eyes with CRVO may provide easily identifiable biomarkers that can predict visual and anatomical outcomes. Therefore, the purpose of this study was to correlate the level and location of retinal hemorrhage in eyes with CRVO with visual and anatomical parameters at baseline and follow-up.

Methods

This retrospective observational study was approved by the Institutional Review Board at the University of California, Los Angeles and adhered to the Health Insurance Portability and Accountability Act (HIPAA) and was performed in accordance with the Declaration of Helsinki. Patients were evaluated at multiple international tertiary care centers (with which the co-authors are affiliated) between January 1, 2010, and September 30, 2019. Co-authors determined respective IRB requirements and provided de-identified clinical datasets and imaging.

Inclusion criteria were comprised of a clinical diagnosis of acute treatment naïve CRVO rendered by the referring retinal specialist based on clinical examination, spectral domain-optical coherence tomography (SD-OCT), and fluorescein angiography (FA). Patients were included if they had a minimum of three months of follow-up with baseline color fundus photography, FA, and SD-OCT volume scans through the central macular region. Acute CRVO was confirmed based on color fundus photography and FA showing the presence of four quadrants of retinal hemorrhages with retinal venous dilation, congestion, and tortuosity, and delayed arterio-venous dye transit (at least 20 seconds) within one month of symptoms onset. Eyes were excluded if they had a concomitant central retinal artery occlusion, evidence of a branch or hemi-central retinal vein occlusion, moderate or severe non-proliferative diabetic retinopathy, proliferative diabetic retinopathy, or significant vitreous hemorrhage preventing fundus photography.

All patients underwent comprehensive ophthalmic assessment including slit-lamp biomicroscopy, indirect ophthalmoscopy, and multimodal retinal imaging. Color fundus photography was performed using a conventional fundus photography camera (Carl Zeiss Meditec, Dublin California, USA; or Topcon, Tokyo, Japan) or an ultra-widefield system (Optos Panoramic 200MA, California, USA; Optos PLC, Dunfermline, Scotland, UK). SD-OCT scans (Spectralis HRA, Heidelberg Engineering; Cirrus HD-OCT 4000, V.5.0, Carl Zeiss Meditec) and fluorescein angiography (Topcon TRC-50; Spectralis HRA, Heidelberg Engineering; Carl Zeiss Meditec; Optos PLC) were captured on all patients. All OCT images were exported to ImageJ (Version 2.0.0-rc-69/1.52p) and scaled according to the built-in scale ledger. Central foveal point thickness (CFT) was manually measured at the central fovea from the internal to the external limiting membrane in order to minimize variability of thickness measurements between OCT machines. Additional clinical data collected for each patient included age, sex, past medical history, systemic medications, and treatment history (i.e. details regarding therapy with intravitreal anti–vascular endothelial growth factor (VEGF) injections, intravitreal steroids, or panretinal photocoagulation (PRP) laser). Therapeutic choice and frequency of administration were determined by the treating provider. Treatment indications were consistent across institution. PRP was performed to target peripheral retinal ischemia, anti-VEGF injections were administered for the treatment of cystoid macular edema

(CME) or subretinal fluid (SRF) or neovascularization of the iris (NVI) or neovascular glaucoma (NVG), and intravitreal steroids were administered for the treatment of macular edema.

Retinal layer depth and location of hemorrhage were determined based on color fundus photography and FA analysis at presentation. Nerve fiber layer (NFL) hemorrhages were defined as hemorrhages that displayed a flame shape and/or radiated within the NFL and/or obscured larger retinal vessels. Hemorrhages were considered deep if they were noted beneath the superficial retinal vasculature with a round shape. Presence of more than two non-contiguous hemorrhages at a given level in the designated region was considered abnormal. Regional localization of the hemorrhages within the peripapillary and perivascular regions was defined as follows. The peripapillary region was defined as a 1-disc diameter area from the optic disc margin. The perivascular region of hemorrhages referred to hemorrhages radiating along the NFL radiations along the major temporal arcades. Specifically, we identified these hemorrhages approximately 1.5 mm–4.5 mm from the optic disc. The temporal border was assessed clinically by placing a vertical line transecting the fovea. Analysis was performed comparing these three groups of increasing severity of hemorrhage (from least to greatest): deep hemorrhages alone, deep hemorrhages and peripapillary NFL hemorrhages (peripapillary group), and deep hemorrhages and peripapillary and perivascular NFL hemorrhages (perivascular group).

Presence of neovascularization of the iris (NVI), neovascular glaucoma (NVG), and vitreous hemorrhage (VH) were determined by the treating provider. Hemorrhage location and extent of ischemia was graded by the first author (AA) based on color and FA images submitted by the referring coauthors and based on the widest view provided. A second grader masked to all clinical data was asked to determine location of hemorrhage and presence/absence of ischemia (AH, JS, FG, DW, CG). Discrepancies were determined by a senior arbiter (DS). Ischemia was defined as greater than 10 disc areas (DA) of non-perfusion present on fluorescein angiography on the widest available view provided, including outside the seven standard fields.[4,21,22] In eyes with multiple FAs, the final FA was used to determine the extent of ischemia. Eyes with confluent hemorrhages that obscured assessment of ischemia or without widefield imaging were eliminated from the ischemia analysis. Presence or absence of CME or SRF was determined based on evaluation of the sub-foveal SD-OCT B-scan.

Statistical analyses were performed using R version 3.5.0 (www.r-project.org). Demographic parameters were reported as mean and standard deviations or numerical counts with percentages. Analysis of ischemic outcomes by hemorrhage level and location was presented as numerical counts and percentages. Snellen visual acuities were converted to logMAR for statistical analysis. Vision was reported as mean and median logMAR vision with Snellen conversion. Central foveal thickness was reported as mean and standard deviations. Comparison of continuous variables was performed with analysis of variance with post-hoc Tukey HSD between the three groups. Pearson's correlation was performed between CFT and baseline or final visual acuity. Cohen's Kappa statistic was calculated for inter-grader reliability. Bonferroni correction was implemented when post-hoc Chi-squared tests were performed between three groups. In these cases $P < 0.016$ (0.05/3). Otherwise, P values < 0.05 were considered significant.

Results

Demographics and Treatment History of the Entire Cohort

A total of 108 eyes with CRVO from 108 patients were included and analyzed. Contribution of cases by each institution is summarized in Supplementary Table S1. At baseline, 37 eyes displayed deep retinal hemorrhages only, 21 eyes displayed deep retinal hemorrhages plus peripapillary NFL (nerve fiber layer) hemorrhages, and 50 eyes displayed deep hemorrhages plus peripapillary and perivascular NFL hemorrhages. An example of a case of CRVO with deep hemorrhages alone (Fig. 1), peripapillary NFL hemorrhages (Fig. 2), and perivascular NFL hemorrhages (Fig. 3) are shown. None of the patients presented with peripapillary or perivascular hemorrhages alone. Cohen's κ for inter-grader reliability was 0.76 (0.63–0.88) between graders for distribution of hemorrhage groups.

Average patient age in the total cohort was 63.6 ± 16.1 years of age and predominantly male (66/108 or 61.1%) with a predilection for the right eye 79/108 (73.1%) (Table 1). Average follow-up period was 17.2 ± 19.2 months (range 2.8 to 105.3 months). In total, 87.0% (94/108) of the patients received at least one anti-VEGF injection (mean 8.5 ± 9.3 injections, range 1–50), 3.7% (4/108) received intravitreal steroids, and 6.5% (7/108) received PRP laser therapy. No patients received intravitreal steroids as first line therapy. Of the four patients with intravitreal steroids, one received three Ozurdex injections, one received five Ozurdex injections, and the other two received one Ozurdex and one Kenalog injection during follow-up. Eyes with only deep retinal hemorrhages (26/37, 70.3%) were significantly less likely to have received anti-VEGF injections compared to eyes with peripapillary (21/21, 100.0%, $P = 0.006$) and perivascular NFL hemorrhages (47/50, 94.0%, $P = 0.003$). No difference in anti-VEGF frequency existed between the perivascular and peripapillary hemorrhage groups ($P = 0.25$). When comparing the rate of anti-VEGF injection over the entire follow-up, patients with only deep hemorrhages underwent 0.5 ± 0.3 injections per month, patients with deep retinal hemorrhages plus peripapillary NFL hemorrhages received 0.9 ± 0.9 injections per month, and patients with deep retinal hemorrhages plus peripapillary and perivascular NFL hemorrhages underwent 0.8 ± 0.9 injections per month ($P = 0.20$).

Correlation Between Baseline NFL Hemorrhage Pattern and Baseline and Final Visual Acuity

Visual outcomes were compared in eyes with hemorrhages involving the NFL versus eyes without hemorrhage in the NFL at baseline presentation (Table 2). Baseline visual acuity in the group with deep retinal hemorrhages alone was 20/100, and in the group with peripapillary NFL hemorrhages it was 20/63, and in the group with perivascular NFL hemorrhages it was 20/200 ($P < 0.003$). Post-hoc Tukey's HSD analysis showed that the significant difference in baseline visual acuity was between the peripapillary and perivascular ($P = 0.002$) groups and the deep and perivascular groups ($P = 0.005$) but not between the deep and peripapillary hemorrhage group ($P = 0.78$). However, at final follow-up there was a graded effect in average visual acuity. Eyes with deep hemorrhages alone improved to 20/40, eyes with peripapillary NFL hemorrhages stabilized at 20/80, and eyes

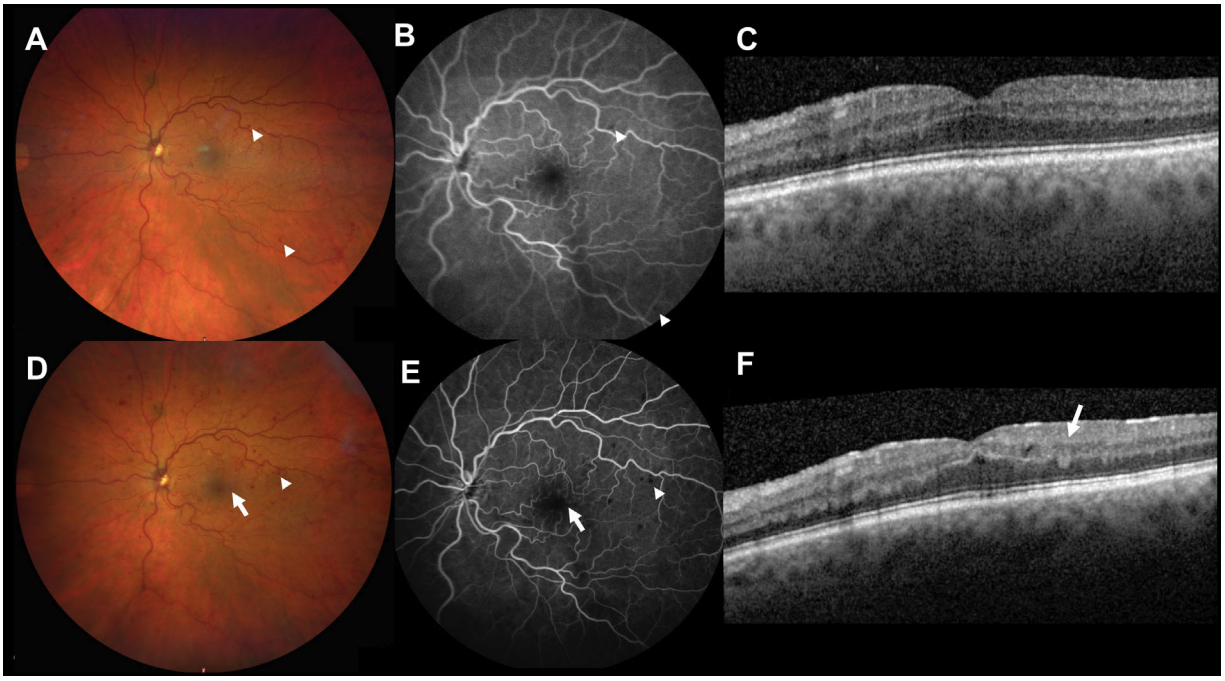

Figure 1. Case 1. Acute CRVO with deep retinal hemorrhages only. Baseline color fundus photograph (A) and fluorescein angiogram (B) show deep retinal hemorrhages in the macula (arrowheads) and no evidence of NFL hemorrhages and no fluid with OCT (C). Follow-up at 3 months demonstrates progressive deep retinal hemorrhages (arrowheads) on color fundus photograph (D) and fluorescein angiogram (E), but still no evidence of NFL hemorrhages. One hemorrhage located in the macula can be identified as deep on OCT (F, arrow). Mild cystic changes were noted on the OCT (F) but no anti-VEGF injection was given. Vision was 20/40 at baseline and last follow-up.

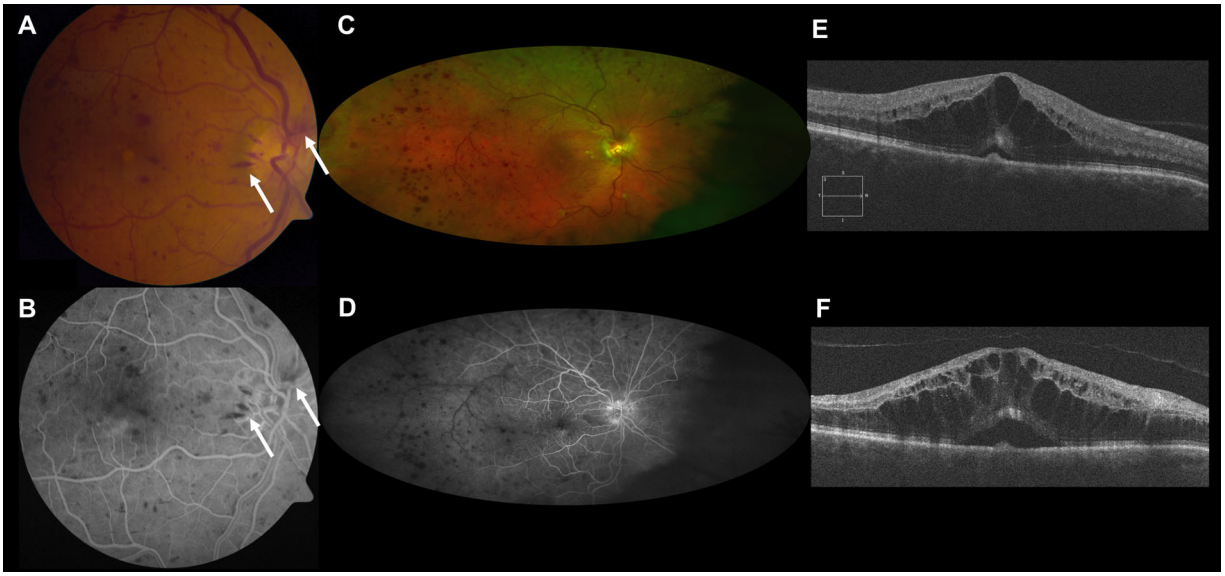

Figure 2. Case 2. Acute CRVO with deep retinal hemorrhages plus peripapillary NFL hemorrhages. Baseline vision was 20/50. Baseline fundus photograph (A) shows superficial NFL hemorrhages in the peripapillary region (arrows) and deep retinal hemorrhages in the macula, which are confirmed on fluorescein angiography (B). At 9 months, follow-up widefield fundus photograph shows persistent deep hemorrhages (C) and follow-up widefield fluorescein angiography illustrates >10 disc areas of nonperfusion, most notably in the temporal retina (D). Baseline SD-OCT (E) shows cystoid macular edema and shallow central subretinal fluid. Follow-up SD-OCT (F) shows persistent CME and SRF despite six bevacizumab injections. Vision worsened to 20/125.

with perivascular NFL hemorrhages demonstrated the lowest VA at 20/100 ($P = 0.03$). Statistical significance occurred between the deep and perivascular hemorrhage group ($P = 0.02$); differences between the peripapillary versus perivascular ($P = 0.49$) and deep versus peripapillary ($P = 0.52$) groups were not significant.

Baseline Hemorrhage Level Correlation with Central Foveal Thickness (CFT) and Fluid Status

Baseline CFT was significantly less in the group with deep hemorrhages alone (455 µm ± 273 µm, $P < 0.001$) and in the group with peripapillary hemorrhages (534 ± 270 µm,

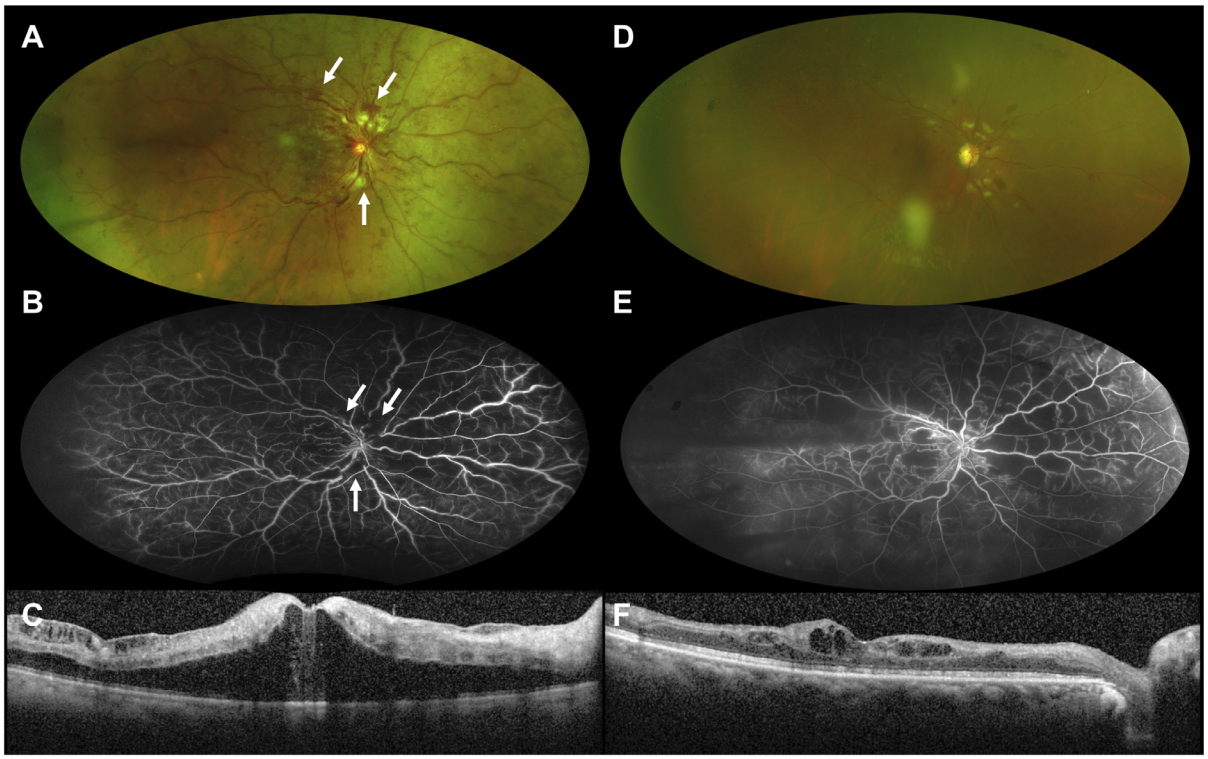

Figure 3. Case 3. Acute CRVO with deep retinal hemorrhages plus peripapillary NFL and perivascular NFL hemorrhages. Widefield fundus photograph at baseline presentation (A) shows flame-shaped NFL hemorrhages in the peripapillary and perivascular regions (arrows) that nearly resolve at the 5-month follow-up visit (D). Widefield fluorescein angiography at baseline (B) demonstrates that the hemorrhages are superficial in a peripapillary and perivascular NFL distribution. Vision at presentation was 20/800. At the 5-month follow-up visit, vision improved to 20/200 but significant (greater than 10 disc areas) diffuse retinal ischemia was noted (E). SD-OCT shows significant central cystoid macular edema at baseline presentation (C) that was much improved at the 5-month follow-up visit (F) after six aflibercept injections.

Table 1. Demographics and Treatment History of Study Population

	Total ($N = 108$)	Deep Hemorrhage Only ($N = 37$)	Deep + Peripapillary NFL ($N = 21$)	Deep + Peripapillary NFL + Perivascular NFL ($N = 50$)	*P* Value
Age (yr, average ± SD)	63.6 ± 16.1	61.5 ± 18.3	68.0 ± 13.3	63.4 ± 15.4	0.35
Sex					
Male, *n* (%)	66 (61.1)	18 (48.6)	15 (71.4)	33 (66.0)	0.15
Female, *n* (%)	42 (38.9)	19 (51.4)	6 (28.6)	17 (34.0)	
Eye					
OD, *n* (%)	79 (73.1)	31 (83.8)	15 (71.4)	33 (66.0)	0.18
OS, *n* (%)	29 (26.9)	6 (16.2)	6 (28.6)	17 (34.0)	
Follow-up (mo, average ± SD)	17.2 ± 19.2	20.4 ± 23.7	20.0 ± 20.0	13.6 ± 14.4	0.19
Received anti-VEGF treatment, *n* (%)	94 (87.0)	26 (70.3)	21 (100.0)	47 (94.0)	<0.001
Injections/total follow-up (injections/mo, average ± SD)	0.7 ± 0.8	0.5 ± 0.3	0.9 ± 0.9	0.8 ± 09	0.20
Intravitreal steroids, *n* (%)	4 (3.7)	0 (0.0)	2 (9.5)	2 (4.0)	0.21
Panretinal photocoagulation, *n* (%)	7 (6.5)	1 (2.7)	1 (4.8)	5 (10.0)	0.37

NFL, nerve fiber layer; SD, standard deviation; VEGF, vascular endothelial growth factor.

$P = 0.002$) compared to the group with perivascular NFL hemorrhages (826 ± 394 µm). No difference was noted between the groups with deep versus peripapillary hemorrhages ($P = 0.72$) (Table 2). Illustrations of the correlation of CME and CFT are shown in Figures 1C (absent CME in a CRVO case with only deep hemorrhages), 2E (baseline CFT of 774 in a CRVO case with peripapillary NFL hemorrhage) and 3C (baseline CFT of 912 in a CRVO case with perivascular NFL hemorrhages). There was a correlation between baseline CFT and baseline visual acuity ($r = 0.45$, $P < 0.001$) and final visual acuity ($r = 0.24$, $p = 0.01$) across all groups.

Cystoid macular edema was present in 64.9% (24/37) of CRVO eyes with deep retinal hemorrhages alone, 81.0% (17/21) of eyes with deep retinal hemorrhages and peripapillary NFL hemorrhages, and 86.0% (43/50) of eyes with deep

Table 2. Vision Outcomes by Hemorrhage Distribution and Depth

	Total ($N = 108$)	Deep Hemorrhage Only ($N = 37$)	Deep + Peripapillary NFL ($N = 21$)	Deep + Peripapillary NFL + Perivascular NFL ($N = 50$)	*P* Value
Baseline vision (logMAR, average ± SD, median, Snellen equivalent)	0.8 ± 0.5, 0.8 (20/126)	0.7 ± 0.5, 0.7 (20/100)	0.6 ± 0.7, 0.5 (20/63)	1.0 ± 0.5, 1.0 (20/200)	0.003
Final vision (logMAR, average ± SD, median, Snellen equivalent)	0.7 ± 0.7, 0.6 (20/80)	0.5 ± 0.5, 0.3 (20/40)	0.7 ± 0.5, 0.6 (20/80)	0.9 ± 0.8, 0.7 (20/100)	0.03
Baseline central foveal thickness (µm, average ± SD, median)	640 ± 358	455 ± 273	534 ± 270	826 ± 394	<0.001

NFL, nerve fiber layer; SD, standard deviation.

Table 3. Anatomical Outcomes Associated with Hemorrhage Location

	Total ($N = 108$)	Deep Hemorrhage Only ($N = 37$)	Deep + Peripapillary NFL ($N = 21$)	Deep + Peripapillary NFL + Perivascular NFL ($N = 50$)	*P* Value
Ischemia >10 DA of nonperfusion, *n* (%)*	38 (46.3)	5 (16.1)	5 (31.3)	28 (80.0)	<0.001
No ischemia <10 DA of nonperfusion, *n* (%)*	44 (53.7)	26 (83.9)	11 (68.7)	7 (20.0)	
NVI, *n* (%)	4 (3.7)	0 (0.0)	3 (14.3)	1 (2.0)	0.01
NVG, *n* (%)	1 (0.9)	0 (0.0)	0 (0.0)	1 (2.0)	–
PRH, *n* (%)	11 (10.2)	3 (8.1)	1 (4.8)	7 (14.0)	0.44
VH, *n* (%)	4 (3.7)	2 (5.4)	1 (4.8)	1 (2.0)	0.68
CME, *n* (%)	84 (77.8)	24 (64.9)	17 (81.0)	43 (86.0)	0.03
SRF, *n* (%)	42 (38.9)	11 (29.7)	11 (52.4)	20 (40.0)	0.23

DA, disc areas; NFL, nerve fiber layer; NVI, neovascularization of the iris; NVG, neovascular glaucoma; PRH, preretinal hemorrhage; VH, vitreous hemorrhage; CME, cystoid macular edema; SRF, subretinal fluid. *Due to a lack of widefield FA or blockage from hemorrhage, eyes in the total (N=82), deep hemorrhage only (N=31), deep + peripapillary NFL (n=16), deep + peripapillary NFL + perivascular NFL (n=35) groups are reduced. Percentages and statistical tests reflect these reduced number.

retinal hemorrhages and peripapillary and perivascular NFL hemorrhages ($P = 0.03$, Table 3). Post-hoc χ^2 tests demonstrated that these differences were primarily between the groups with deep and perivascular NFL hemorrhages that did not reach significance with the conservative Bonferroni correction ($P = 0.02$). Subretinal fluid was present in 29.7% (11/37) of eyes with deep retinal hemorrhages alone, 52.4 % (11/21) of eyes with peripapillary NFL hemorrhages, and 40.0% (20/50) of eyes with perivascular NFL hemorrhages ($P = 0.23$) (Table 3).

Baseline Hemorrhage Level Correlation with Ischemic Outcomes

In total, 26 of the 108 eyes were excluded only as pertains to the ischemic evaluation due to lack of widefield imaging or blockage from hemorrhage. Specifically this occurred in 6 eyes in the deep (n=31), 5 eyes in the peripapillary (n=16), and 15 eyes in the perivascular (n=35) groups. In total, 38 (46.3%) eyes displayed >10 disc areas of ischemia (i.e., ischemic CRVO), whereas 44 (53.7%) eyes were considered nonischemic CRVO. Ischemic CRVO was identified in 16.1% (5/31) of eyes with deep hemorrhages alone, 31.3% (5/16) of eyes with peripapillary NFL hemorrhages, and 80.0% (28/35) of eyes with perivascular NFL hemorrhages ($P < 0.001$) (Table 3). Please see Figures 2D, 3B, and 3E for case examples. Post-hoc χ^2 tests illustrated continued statistical significance between the peripapillary versus perivascular ($P = 0.001$) and deep versus perivascular ($P < 0.001$) groups but not between the deep versus peripapillary groups ($P = 0.23$). In the 39 eyes with less than 6-month follow-up, 0/13 (0.0%) in the deep hemorrhage alone group, 1/5 (20.0%) in the peripapillary group, and 14/21 (66.7%) in the perivascular group illustrated evidence of ischemic CRVO. Of those eyes with NVI (a total of four of 108 eyes), three were in the peripapillary NFL hemorrhage group and one was in the perivascular NFL hemorrhage group. Only one eye in the entire cohort developed NVG, and this eye showed perivascular NFL hemorrhages. Eyes with preretinal hemorrhages were less likely to show deep hemorrhages alone (3/37, 8.1%) versus the group with perivascular NFL hemorrhages (7/50, 14.0%), but this was not statistically significant ($P = 0.44$).

Discussion

This study evaluated the depth and pattern of distribution of retinal hemorrhages at presentation as a potential biomarker for visual and anatomic outcomes in patients with acute CRVO. Eyes with baseline retinal hemorrhages in a perivascular NFL distribution i.e. radial extension of the hemorrhages along the temporal vascular arcades exhibited significantly worse baseline and final visual acuities, a greater prevalence and severity of cystoid macular edema, a greater frequency of ischemic CRVO (versus nonischemic CRVO), and a greater rate of anti-VEGF injection therapy.

Other known biomarkers of ischemic CRVO have been described and include baseline visual acuity, relative afferent pupillary defect, cotton wool spots and extent of retinal hemorrhages.[1,2,4] From the CVOS, nonperfusion of greater than 10 disc areas with FA was a key risk factor for neovascularization.[4,22] In fact, Nicholson et al.[5] demonstrated that

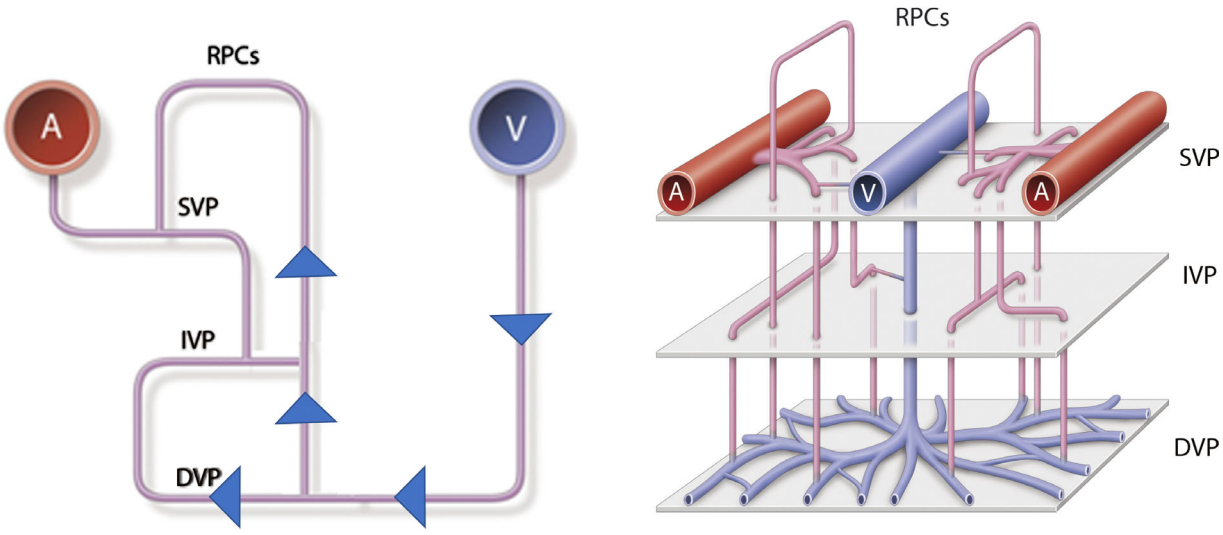

Figure 4. Diagram illustrating proposed cascade or progression of increased venous pressure leading to the distribution of retinal hemorrhages. Hemorrhages are first noted at the level of the deep retinal capillary plexus (DCP), the major level of venous outflow, in the posterior pole and periphery.[8,9,11,14,19,20] Pressure will subsequently be transmitted in more severe forms of CRVO through the intermediate capillary plexus (IVP), the superficial capillary plexus (SCP) and ultimately to the RPC.[28,33,38] Therefore, hemorrhages within the RPC NFL may indicate a more severe form of CRVO. Reprinted with permission from Fouquet S, Vacca O, Sennlaub F, Paques M. The 3D retinal capillary circulation in pigs reveals a predominant serial organization. *Invest Ophthalmol Vis Sci.* 2017;58:5754–5763. © 2017 The Authors. Published by the Association for Research in Vision and Ophthalmology (ARVO).

ischemia or nonperfusion area of 75 to 150 disc areas was associated with an 80% rate of neovascularization. Tsui et al.[23] confirmed that eyes with a nonperfused area or ischemic index of 45% of the total retina area were at a significantly greater risk of neovascularization. Hayreh et al.[2] evaluated the pattern of retinal hemorrhages in acute CRVO and found that 92% of patients with ischemic CRVO displayed peripapillary hemorrhages versus 71% of eyes with nonischemic CRVO at baseline. In addition, 47% of the eyes with ischemic CRVO versus 16% with nonischemic CRVO displayed severe hemorrhages in the peripapillary area. Although the Hayreh study did not use 10 disc areas of nonperfusion to define an ischemic CRVO and did not evaluate or identify depth of hemorrhage as a risk factor, his findings are consistent with the results of our study suggesting that perivascular NFL hemorrhages portend a worse anatomic and visual outcome. However, it should be noted that the definition of 10 DA as a critical margin for ischemia differs from that which was originally described in CVOS, as this was defined in relationship to the standard seven fields.[4,22] Furthermore, 10 DA of ischemia was arbitrarily determined and not considered a step-up in risk.

The development of retinal hemorrhages and ischemia may have a common pathophysiology in eyes with CRVO. A thrombus in the central retinal vein, most commonly located posterior to the lamina cribosa, may initiate a cascade of events including increased hydrostatic pressure within the retinal venous system that is transmitted from the venous pole to the terminal arterioles.[24,25] Middle retinal infarction at the level of the inner nuclear layer, identified as PAMM on SD-OCT and perivenular PAMM with en face OCT, may be the first manifestation of ischemic injury in eyes with CRVO.[8–12] In more severe cases, ischemia progresses towards the arterial pole leading to inner retinal ischemia. This is detected on SD-OCT as hyperreflectivity of the inner and middle retina. This has been termed the ischemic cascade.[15] The development of retinal hemorrhages may show a similar sequence of progression.

In patients with elevated retinal venous pressure due to local and systemic etiologies, retinal hemorrhages may be identified only in the Henle fiber layer.[16–18,39] This suggests that the intermediate and deep retinal capillary plexus may be the major site of venous outflow and may be at greatest risk of ischemia and hemorrhage.[19,20] In more severe cases, ischemia and hemorrhage may track superficially into the inner retina, and as suggested by this study, extend into the radial peripapillary capillary plexi (RPC) within the NFL. This is mainly in an area radiating away from the disc where the NFL is thickest and the RPC is present; more peripheral, the RPC is absent and only deep retinal hemorrhages are seen.[26,27]

The organization of the retinal capillary plexus has been extensively studied but the exact arrangement, specifically the nature of the venous drainage, has not been clearly elucidated.[20] Fouquet et al.[28] have illustrated a serial arrangement of the retinal microvasculature in which the RPC drains directly into the DCP and subsequently empties into a postcapillary venule in pigs (Fig. 4). This has been confirmed in other mammals and in humans.[20,29–32] More recent human ex vivo studies, however, contradict this pattern of venous drainage.[33] Our findings suggest that in eyes with CRVO, the ICP and DCP (closest to the draining venules) may be at greatest risk of injury from increased hydrostatic pressure while the SCP and the RPC may be more resistant. Thus hemorrhage and ischemia will develop first in the region of the ICP and DCP and with more severe occlusion, hemorrhage and ischemia will be evident in the superficial capillary plexus and ultimately the RPC NFL.[8–12,34] This pathway may explain the salient finding of this study, which identified RPC NFL hemorrhages, particularly along the radial perivascular extensions, as a biomarker of a more severe phenotype of CRVO with worse visual outcomes and increased retinal ischemia and cystoid macular edema.

This pathway may also explain why patients with more severe CRVO display more extensive retinal hemorrhages. The extent of hemorrhage is a commonly accepted biomarker for ischemic CRVO but its identification lacks the mechanistic understanding this paper provides.[2,22] Further, it is important to note that in this study NFL hemorrhage correlated not only with greater ischemia but also with worse visual outcomes, greater central macular thickness, and greater prevalence and severity of CME and increased rate of treatment with anti-VEGF. This would indicate that NFL hemorrhages correspond to outcomes beyond ischemia that strengthen its independence from extent of hemorrhages.

An unexpected finding of our study is the predilection of acute CRVO in the right eye across the entire cohort of patients. We speculate that this may be due to the unique anatomy of the right internal jugular vein which connects directly with the SVC or superior vena cava (the left internal jugular vein is separated from the SVC by the innominate vein) leading to greater venous pressures on the right side. As the right atrium fills during diastole against a closed tricuspid valve, the pressure increases due to increased blood volume. This pressure is likely exacerbated in patients with chronic hypertension who have hypertrophic myocardium, stiffened vessels, or sclerotic or incompetent tricuspid valve. As a result, this increases retrograde pressure that can be transmitted to the superior ophthalmic vein and potentially the central retinal vein. This has been supported by studies that have demonstrated a larger right than left internal jugular vein by ultrasound or CT scan.[35–37]

Limitations of this study include the retrospective design, the nonstandardized imaging protocols, and the variable follow-up which prevented uniform analysis of all eyes. As ischemia was considered within and outside the standard seven fields, bias may have been introduced as areas of the peripheral retina may not have been appropriately captured in all cases. The heterogenous follow-up made it difficult to assess subtle changes in visual acuity and the relative impact of anti-VEGF therapy efficacy and its effect on macular edema and neovascularization. The development of neovascularization of the iris or neovascular glaucoma may have been masked by anti-VEGF therapy given for coexistent cystoid macular edema. Furthermore, the extent of ischemia can change over time and can be masked by blockage from hemorrhage on fluorescein angiography. Additional systemic factors (e.g. anticoagulation, blood pressure) may have influenced the extent and severity of hemorrhages and may have also confounded our findings. Last, the study was underpowered to statistically evaluate for trends that were not significant, such as the number of injections performed per month. Future prospective longitudinal studies with a standardized imaging protocol and a natural history control cohort will be necessary to formally validate the findings of this study. However, this investigation may serve as a pilot study to be further validated with larger prospective data sets that include uniform multimodal retinal imaging.

In conclusion, we provide evidence that in CRVO patients, eyes with retinal hemorrhages located in the RPC NFL, specifically along the major vascular arcades, may represent more severe forms of CRVO with worse visual outcomes, increased cystoid macular edema, and greater risk of ischemic complications. As such, perivascular NFL hemorrhage radiating along the vascular arcades may provide an easily identifiable biomarker of ischemic CRVO at greater risk for iris and angle neovascularization and with more adverse visual and anatomical outcomes.

Acknowledgments

Supported by Research To Prevent Blindness Inc., New York, New York (DS) and The Macula Foundation Inc., New York, New York (DS, KBF).

Disclosure: **A. Au,** None; **A. Hilely,** None; **J. Scharf,** None; **F. Gunnemann,** None; **D. Wang,** None; **I. Chehaibou,** None; **C. Iovino,** None; **C. Grondin,** None; **M.-L. Farecki,** None; **K. G.Falavarjani,** None; **N. Phasukkijwatana,** None; **M Battista,** None; **E. Borrelli,** Centervue (R), Carl Zeiss Meditec (R); **R. Sacconi,** Carl Zeiss Meditec (R); **B. Powell,** None; **G. Hom,** None; **T.E. Greenlee,** None; **T.F. Conti,** None; **G. Ledesma-Gil,** None; **M.Y. Teke,** None; **N. Choudhry,** Topcon (C, F, R), Optos (C, F, R), Bayer (C, F, R), Allergan (C, R), Novartis (C), Carl Zeiss Meditec (C, F, R), Ellex (C); **A.T. Fung,** Allergan (C) Bayer (C); **V. Krivosic,** Novartis (F), Bayer (F), Allergan (F); **J. Baek,** None; **M.Y. Lee,** None; **Y. Sugiura,** None; **G. Querques,** Alimera Sciences (C), Allergan (C), Amgen (C), Bayer (C), Heidelberg (C), KBH (C), LEH Pharma (C), Lumithera, Novartis (C), Sandoz (C), Sifi (C), Sooft-Fidea (C), Carl Zeiss Meditec (C); **E. Peiretti,** Bayer (C), Novartis (C) Sifi (R), Allergen (R), Baush and Lomb (R); **R. Rosen,** OptoVue (C, P); GlaucoHealth (I); Regeneron, Bayer (C), OD-OS (C), NanoRetina (C), Genetech-Roche (C), Boehringer-Ingelheim (C), Astellas (C), Teva (C); **W.K. Lee,** Bayer (F), Novartis (F); **L.A. Yannuzzi,** None; **D. Zur,** Allergan (C), Bayer (C); **A. Loewenstein,** Allergan (C), Novartis (C), Genentech-Roche (C), Notal Vision (C), Forsightslabs (C), Beyeonics (C), Bayer (C); **D. Pauleikhoff,** Genentech-Roche (C), Novartis (C, F), Bayer (C, F); **R. Singh,** Novartis (C), Bayer (C), Regeneron (C), Carl Zeiss Meditec (C), Bausch and Lomb (C), Genentech-Roche (C); Graybug (F), Apellis (F); **Y. Modi,** None; **J.P. Hubschman,** Alcon (C), Allergan (C), Bausch-Lomb (C), Allergan (S), Novartis (S); **M. Ip,** Thrombogenics (C), Boehringer Ingelheim (C), RegenexBio (C), Amgen (C), Novartis (C), Allegro (C), Allergan (C), Lineage Cell Therepeutics (C), Clearside (C), Genentech (C); **S. Sadda,** Allergan (C), Amgen (C), Regeneron (C), Bayer (C), Genentech-Roche (C), Novartis (C), 4DMT (C), Optos (C, F), Heidelberg (C, F), Centervue (C, F), Topcon (F), Nidek (F), Carl Zeiss (F); **K.B. Freund,** Genentech-Roche (C), Optovue (C), Carl Zeiss Meditech (C), Heidelberg (C), Allergan (C), Bayer (C), Novartis (C), Genentech-Roche (F); **D. Sarraf,** Amgen (C, F), Genetech-Roche (C, F), Heidelberg (F), Novartis (C, F), Optovue (C,F), Regeneron (F), Bayer (C,F), Topcon (F)

References

1. Hayreh SS, Klugman MR, Beri M, Kimura AE, Podhajsky P. Differentiation of ischemic from non-ischemic central retinal vein occlusion during the early acute phase. *Graefe's Arch Clin Exp Ophthalmol*. 1990;228:201–217.
2. Hayreh SS, Zimmerman MB. Fundus changes in central retinal vein occlusion. *Retina*. 2015;35:29–42.
3. Hayreh SS. The CVOS Group M and N reports. *Ophthalmology*. 1996;103:350–352.
4. Hayreh SS, Podhajsky PA, Zimmerman MB, Clarhson JC. Natural history and clinical management of central retinal vein occlusion. *Arch Ophthalmol*. 1997;115:486–491.
5. Nicholson L, Vazquez-Alfageme C, Patrao V, et al. Retinal nonperfusion in the posterior pole is associated with increased risk of neovascularization in central retinal vein occlusion. *Am J Ophthalmol*. 2017;182:118–125.
6. Thomas AS, Thomas MK, Finn AP, Fekrat S. Use of the ischemic index on widefield fluorescein angiography to characterize a central retinal vein occlusion as ischemic or nonischemic. *Retina*. 2019;39:1033–1038.

7. Tan CS, Chew MC, van Hemert J, Singer MA, Bell D, Sadda SR. Measuring the precise area of peripheral retinal nonperfusion using ultra-widefield imaging and its correlation with the ischaemic index. *Br J Ophthalmol*. 2016;100:235–239.
8. Rahimy E, Kuehlewein L, Sadda SR, Sarraf D. Paracentral acute middle maculopathy: what we knew then and what we know now. *Retina*. 2015;35:1921–1930.
9. Chen X, Rahimy E, Sergott RC, et al. Spectrum of retinal vascular diseases associated with paracentral acute middle maculopathy. *Am J Ophthalmol*. 2015;160:26–34.e1.
10. Yu S, Pang CE, Gong Y, et al. The spectrum of superficial and deep capillary ischemia in retinal artery occlusion. *Am J Ophthalmol*. 2015;159:53–63.e2.
11. Rahimy E, Sarraf D, Dollin ML, Pitcher JD, Ho AC. Paracentral acute middle maculopathy in nonischemic central retinal vein occlusion. *Am J Ophthalmol*. 2014;158:372–380.e1
12. Sarraf D, Rahimy E, Fawzi AA, et al. Paracentral acute middle maculopathy: a new variant of acute macular neuroretinopathy associated with retinal capillary ischemia. *JAMA Ophthalmol*. 2013;131:1275–1287.
13. Ghasemi Falavarjani K, Phasukkijwatana N, Freund KB, et al. En face optical coherence tomography analysis to assess the spectrum of perivenular ischemia and paracentral acute middle maculopathy in retinal vein occlusion. *Am J Ophthalmol*. 2017;177:131–138.
14. Nemiroff J, Phasukkijwatana N, Sarraf D. Optical coherence tomography angiography of deep capillary ischemia. *Developments in Ophthalmology*. 2016;56:139–145.
15. Bakhoum MF, Freund KB, Dolz-Marco R, et al. Paracentral acute middle maculopathy and the ischemic cascade associated with retinal vascular occlusion. *Am J Ophthalmol*. 2018;195:143–153.
16. Au A, Hou K, Baumal CR, Sarraf D. Radial hemorrhage in Henle layer in macular telangiectasia type 2. *JAMA Ophthalmol*. 2018;136:1182–1185.
17. Agarwal A, Gass JDM. *Gass' Atlas of Macular Diseases*. 5th ed. St Louis: Mosby: Elsevier Saunders; 2012;1–1378.
18. Kon Graversen VA, Jampol LM, Meredith T, et al. Hemorrhagic unilateral retinopathy. *Retina*. 2014;34:483–489.
19. Freund KB, Sarraf D, Leong BCS, Garrity ST, Vupparaboina KK, Dansingani KK. Association of optical coherence tomography angiography of collaterals in retinal vein occlusion with major venous outflow through the deep vascular complex. *JAMA Ophthalmol*. 2018;136:1262–1270.
20. Garrity ST, Paques M, Gaudric A, Freund KB, Sarraf D. Considerations in the understanding of venous outflow in the retinal capillary plexus. *Retina*. 2017;37:1809–1812.
21. McIntosh RL, Rogers SL, Lim L, et al. Natural history of central retinal vein occlusion: an evidence-based systematic review. *Ophthalmology*. 2010;117:1113–1123.e15.
22. The Central Vein Occlusion Study Group. A randomized clinical trial of early panretinal photocoagulation for ischemic central vein occlusion. *Ophthalmology*. 1995;102:1434–1444.
23. Tsui I, Kaines A, Havunjian MA, et al. Ischemic index and neovascularization in central retinal vein occlusion. *Retina*. 2011;31:105–110.
24. Green WR, Chan CC, Hutchins GM, Terry JM. Central retinal vein occlusion: a prospective histopathologic study of 29 eyes in 28 cases. *Trans Am Ophthalmol Soc*. 1981;79:371–422.
25. Michel J. Die spontane Thrombose der Vena centralis des Opticus. *Albr von Græfe's Arch für Ophthalmol*. 1878;24:37–70.
26. Jia Y, Simonett JM, Wang J, et al. Wide-field OCT angiography investigation of the relationship between radial peripapillary capillary plexus density and nerve fiber layer thickness. *Invest Ophthalmol Vis Sci*. 2017;58:5188–5194.
27. Henkind P. Radial peripapillary capillaries of the retina. I. Anatomy: human and comparative. *Br J Ophthalmol*. 1967;51:115–123.
28. Fouquet S, Vacca O, Sennlaub F, Paques M. The 3D retinal capillary circulation in pigs reveals a predominant serial organization. *Invest Ophthalmol Vis Sci*. 2017;58:5754–5763.
29. Paques M, Tadayoni R, Sercombe R, et al. Structural and hemodynamic analysis of the mouse retinal microcirculation. *Invest Ophthalmol Vis Sci*. 2003;44:4960–4967.
30. Snodderly D, Weinhaus R, Choi J. Neural-vascular relationships in central retina of macaque monkeys (Macaca fascicularis). *J Neurosci*. 1992;12:1169–1193.
31. Genevois O, Paques M, Simonutti M, et al. Microvascular remodeling after occlusion-recanalization of a branch retinal vein in rats. *Invest Ophthalmol Vis Sci*. 2004;45:594–600.
32. Foreman DM, Bagley S, Moore J, Ireland GW, McLeod D, Boulton ME. Three dimensional analysis of the retinal vasculature using immunofluorescent staining and confocal laser scanning microscopy. *Br J Ophthalmol*. 1996;80:246–251.
33. Chandrasekera E, An D, McAllister IL, Yu DY, Balaratnasingam C. Three-dimensional microscopy demonstrates series and parallel organization of human peripapillary capillary plexuses. *Invest Ophthalmol Vis Sci*. 2018;59:4327–4344.
34. Hogan MJ, Alvarado JA WJ. *Histology of the Human Eye: An Atlas and Textbook*. Philadelphia, PA: WB Saunders Co.; 1971;1–687.
35. Lim C, Keshava S, Lea M. Anatomical variations of the internal jugular veins and their relationship to the carotid arteries: A CT evaluation. *Australas Radiol*. 2006;50:314–318.
36. Tartière D, Seguin P, Juhel C, Laviolle B, Mallédant Y. Estimation of the diameter and cross-sectional area of the internal jugular veins in adult patients. *Crit Care*. 2009;13:R197.
37. Lobato EB, Sulek CA, Moody RL, Morey TE. Cross-sectional area of the right and left internal jugular veins. *J Cardiothorac Vasc Anesth*. 1999;13:136–138.
38. Zhang HR. Scanning electron-microscopic study of corrosion casts on retinal and choroidal angioarchitecture in man and animals. *Prog Retin Eye Res*. 1994;13:243–270.
39. Baumal CR, Sarraf D, Bryant T, et al. Henle fiber layer hemorrhage: clinical features and pathogenesis. *Br J Ophthalmol*. 2020. In press.